

# 1

## Introduction to Communication System-on-Chip, RF Analog Front-End, OFDM Modulation, and Performance Metrics

### 1.1 Communication System-on-Chip

#### 1.1.1 Introduction

Radio frequency (RF) communication systems use RFs to transmit and receive information such as voice and music with FM, or video with TV, and so on (Steele, 1995; Rappaport, 1996; Haykin, 2001). From a general point of view RF communication is simply composed of an RF transmitter sending the information and an RF receiver recovering the information (Figure 1.1). Below are basic definitions of the vocabulary commonly used in communication systems:

- **Signal:** Information (data, image, music, voice, . . . ) we want to transmit and receive.
- **Carrier frequency:** RF sinusoidal waveform, called a carrier because it is used to “carry” the signal from the transmitter to the receiver.
- **MODulation:** Modifying the carrier waveform in order to convey the information (signal) in transmission.

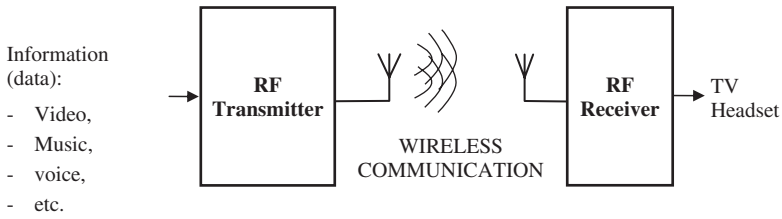


**Figure 1.1** Basic view of an RF communication system

- **DEModulation:** Extracting the signal (i.e., the information) from the carrier frequency in reception.
- **Antenna:** Device which transforms the electrical signal into electromagnetic waves for radiation and vice versa.
- **Channel bandwidth:** Span of frequencies used for the communication.
- **MODEM** = MODulator + DEModulator.
- **TRANSCIVER** = TRANSmitter + reCEIVER.

In the last decades telecommunications have migrated toward digital technology (Proakis, 1995) as a result of the evolution of advanced digital signal processing (DSP) techniques which can now be deployed at low-cost in mobile devices. Nowadays a mobile phone is not only used for traditional voice calls but as a multimedia platform for surfing the Internet, listening to music, data transfers, localization (global positioning system (GPS)), and so on: many applications which require the implementation of different technologies and communication standards (WiFi, Bluetooth, GSM/3G/4G Long Term Evolution (LTE), GPS, near-field communication (NFC), etc.) on the same platform. Since the phone's form factor and battery life are limited, state-of-the-art integrated circuit (IC) design and system-on-chip (SoC) implementations have become necessities for providing cost-effective solutions to the market.

Modern digital communications transceivers (Figure 1.2) are generally composed of a Medium Access Control (MAC) layer managing the access to the medium between different users in a network and the quality of service seen by each, and a PHY (Physical

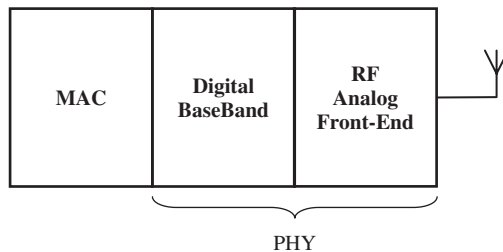


**Figure 1.2** Basic partitioning of a digital communication transceiver

Layer) which is responsible for the transfer of information across the medium (wireless channel, cable, optical fiber, etc.). The PHY can be decomposed into two blocks:

- The digital baseband (DBB) which is located between the MAC and the analog front-end (AFE). The baseband transmission path encodes the bits provided by the MAC, generates the data symbols to be sent across the medium, and finally performs the digital modulation. The reception path demodulates the data and provides a decoded bit stream to the MAC. Generally, the transmission requirements are well specified by the standards (channel coding, modulation, etc.), whereas the algorithms used in reception (channel estimation/equalization, synchronization, etc.) can vary from one implementation to another.
- The RF AFE is connected to the DBB. The RF transmit path converts the DBB signal to analog and frequency up-converts to RF. The receiver frequency down-converts the RF signal to baseband, filters out any interferers, and finally converts the signal to DBB.

### 1.1.2 CMOS Technology

As complementary metal oxide semiconductor (CMOS) technology presents remarkable shrinking properties and cost attractiveness, it has become the unavoidable choice for semiconductors implementing SoC and for low-cost combo-chips integrating several systems on the same die (Abidi, 2000; Brandolini *et al.*, 2005). Although CMOS was initially dedicated to digital design, today RF AFEs are embedded using this technology as well in order to improve the integration efficiency and thus lower the platform cost (Lee, 1998; Razavi, 1998a,b; Iwai, 2000). Nevertheless, CMOS is not well-optimized for RF analog design due to the low ohmic substrate limiting the analog/digital isolation, the low-voltage supply limiting the dynamic range/linearity, and the poor quality factor of the passive components. Furthermore, in deep-submicrometer CMOS technology (nanometer), whereas the digital part of the chip naturally shrinks with the process ratio, the RF analog part scales poorly (Figure 1.3), at around 10% per process node, and generally requires a redesign in order to be able to reduce its area and power consumption. Consequently, for SoC integration the RF AFE remains the major bottleneck in reducing the CMOS transceiver size, therefore requiring more work.

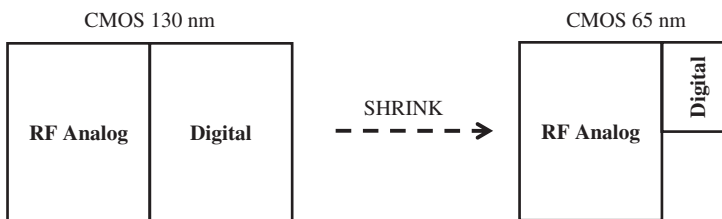


**Figure 1.3** SoC shrink limitation due to the RF analog part of the chip

### 1.1.3 Coexistence Issues

Due to the integration constraints imposed by multi-communication applications, several communication systems often have to coexist on the same platform (such as mobile phone), and in the worst case even on the same chip. Even if the radios do not operate in the same band, any RF transmitter generates broadband out-of-band emissions which can degrade the sensitivity of neighboring receiver bands, as illustrated in Figure 1.4.

If the systems are located on the same platform but not on the same chip, a coupling between antennas, or between chips at the pin level, can occur, as depicted in Figure 1.5. Board design and layout, as well as the distance between the antennas and their orientation, have to be carefully taken into account for limiting the coupling factor between the two systems.

The most difficult case concerns the recent combo-chips, in which the different communication systems are embedded on the same die (Figure 1.6), especially if the power amplifiers (PAs) are also integrated. In addition to the external coupling, on-chip leakage and coupling can pose particular problems because the RF filtering is not present at this level. As with the board design, chip layout and position of the blocks are fundamental design considerations.

Because modern receiver sensitivities are generally specified to be very low for guaranteeing good reception even in weak signal conditions and to relax the transmit power requirements, transmitter out-of-band emissions can rapidly become a real bottleneck if they increase the overall noise floor of the multi-communications system. For example, let us suppose a victim receiver having a bandwidth of 1 MHz and a noise figure of 5 dB; in this case its input-referred noise floor is  $-109$  dBm/MHz ( $kTBF$  at room temperature:  $-174 + 10 \log_{10}(1e6) + 5$ ). By assuming a coupling factor between

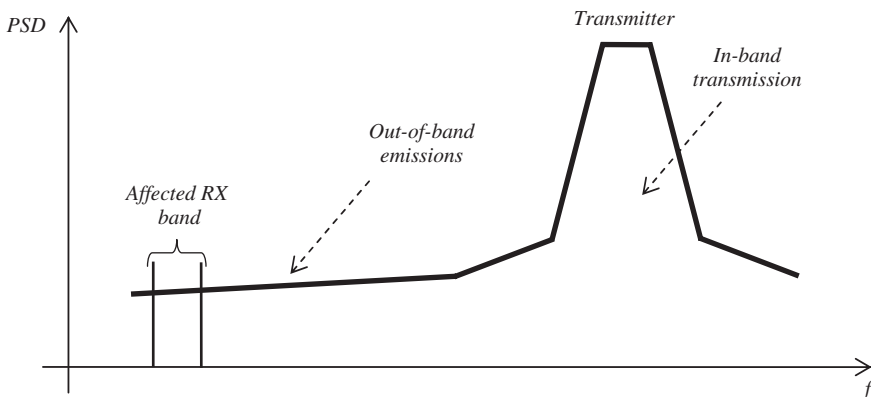


**Figure 1.4** Radio coexistence issues due to transmitter out-of-band emissions

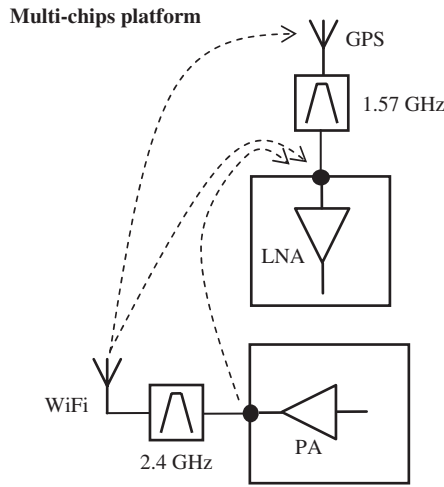


**Figure 1.5** Multi-chips coupling through the antennas

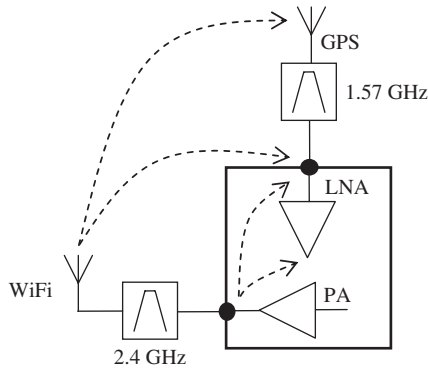


**Figure 1.6** Antennas and systems on-chip coupling

the antennas, we can estimate its sensitivity degradation as a function of the transmitter out-of-band emissions level seen in the receiver band. Figure 1.7 is a plot of the victim receiver sensitivity degradation as function of the transmitter out-of-band emissions assuming a coupling factor of  $-10$  dB between the two antennas. The degradation is negligible, that is, smaller than  $0.1$  dB, if the transmitter out-of-band emissions are lower than  $-115$  dBm/MHz in the receiver bandwidth. The emission specification can be relaxed if we tolerate a higher degradation; for example, the transmitter out-of-band emissions can reach  $-105$  dBm/MHz for an allowed degradation of  $1$  dB.

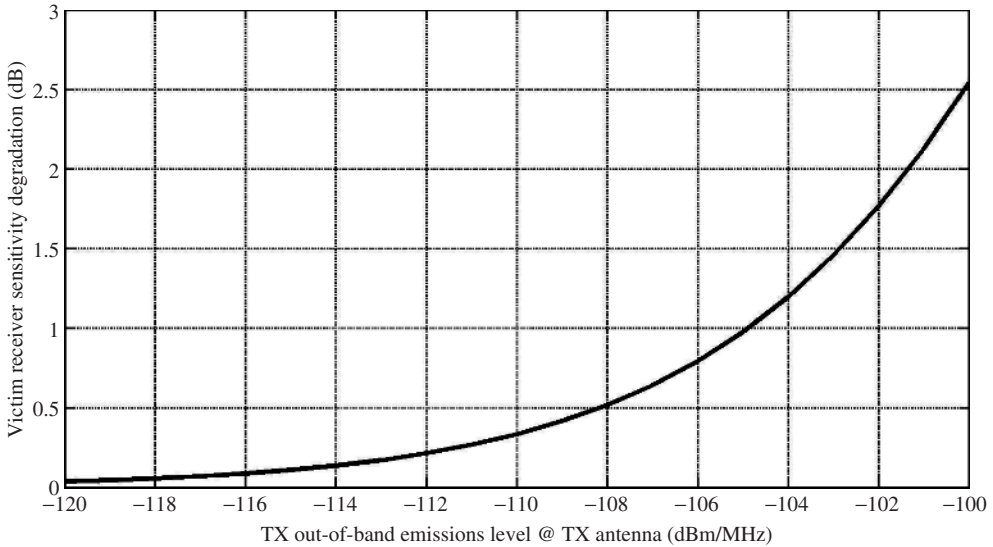


**Figure 1.7** RX sensitivity degradation as a function of the TX out-of-band emissions level by assuming  $-10$  dB coupling factor between the antennas and  $-109$  dBm/MHz receiver noise floor

## 1.2 RF AFE Overview

### 1.2.1 Introduction

In electronics engineering the term “analog signal” comes from the ANALOGY of the signal to continuously vary in time like the underlying physical phenomenon, as opposed to the digital/numerical signal which is discrete and quantized with a certain resolution imposed by the DSP. In modern transceivers the frontier between the analog domain and the digital one is delimited by analog to digital converters (ADCs) and digital to analog converters (DACs) in reception and transmission, respectively, as depicted in Figure 1.8. The RF AFE is composed of two paths, one for receiving the RF signal and the other one for transmitting the baseband signal.

The primary function of an RF analog receiver is to amplify and to frequency down-convert the desired signal from RFs to baseband with minimum degradation. Its main requirements are:

- The frequency band, imposed by the regulation bodies, specifying the local oscillator (LO) frequency range.
- The signal bandwidth specifying the analog baseband filtering.
- The minimum sensitivity specifying the noise figure imposed by the minimum signal-to-noise ratio (SNR) required for good data demodulation.

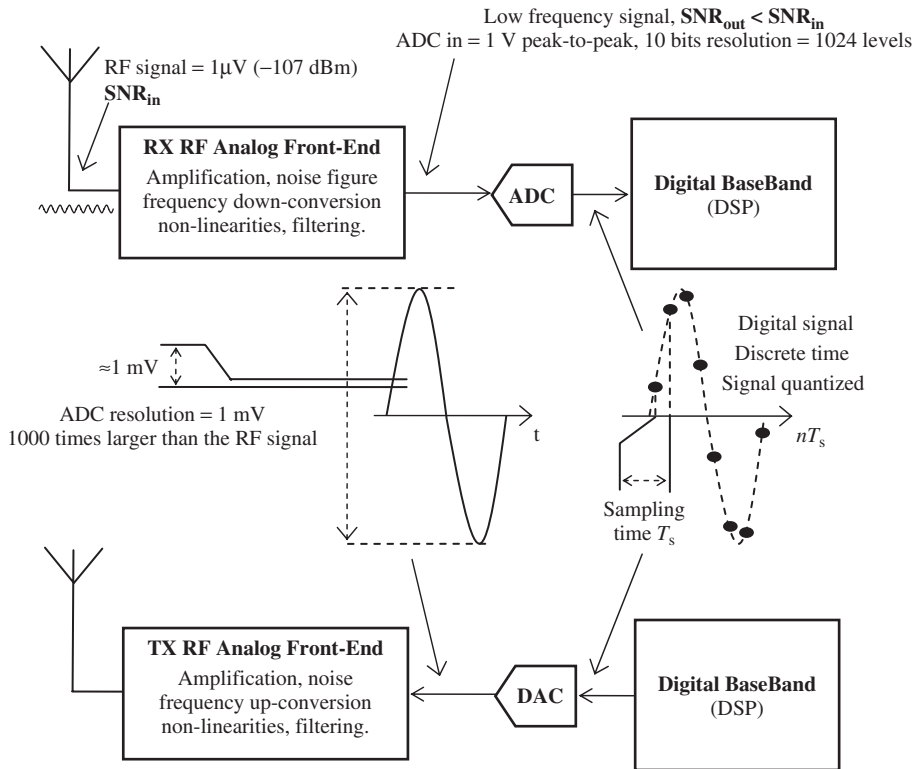


**Figure 1.8** RF analog and DBB partitioning in modern transceivers

- The signal dynamic range specifying the automatic gain control (AGC) design and the ADC resolution.
- The adjacent channel selectivity (ACS) and the blockers/interferer rejection specifying the linearity, the analog baseband filtering, and the LO phase noise profile.

The principal function of an RF analog transmitter is to frequency up-convert the baseband signal to RF and to amplify it to the required transmission power. Its major requirements are:

- The frequency band specifying the LO frequency range.
- The maximum transmission power specifying the PA.
- The error vector magnitude (EVM); that is, modulation accuracy, specifying the noise budget including thermal noise, phase noise, DAC resolution, and linearity.
- The adjacent channel leakage ratio (ACLR) specifying the spectrum emission mask.
- The spurious emission mask specifying the out-of-band unwanted emissions.

Different AFE architectures exist with various advantages and drawbacks, and proper selection depends on the application and performance requirements. We will briefly describe several architectures in the next sections and evaluate their suitability for SoC integration.

### 1.2.2 Superheterodyne Transceiver

The architecture of the superheterodyne transceiver is shown in Figure 1.9. A first RF bandpass filter shared by the reception and the transmission paths limits the overall frequency band to a range of interest.

In reception, after the low-noise amplifier (LNA) fixing the sensitivity with low noise figure and high gain, another RF filter called an image rejection filter is present before the first frequency down-conversion to an intermediate frequency (IF), in order to reject the frequency image which is located at an offset of  $2 \times \text{IF}$  from the channel of interest. This is illustrated in Figure 1.10 with two possibilities for the LO frequency:  $f_{\text{LO}} = f_{\text{channel}} \pm \text{IF}$ . Because the IF is constant regardless of the selected channel, a high selectivity bandpass filter centered on IF can be used in order to attenuate the adjacent channels; this is the strong advantage of the superheterodyne architecture. Afterwards the IF signal is frequency down-converted to baseband with a quadrature mixer and finally digitized by an ADC after anti-alias filtering.

In transmission the channel is first up-converted to IF with a quadrature mixer, then filtered by an IF bandpass filter to remove out-of-band noise, and finally up-converted

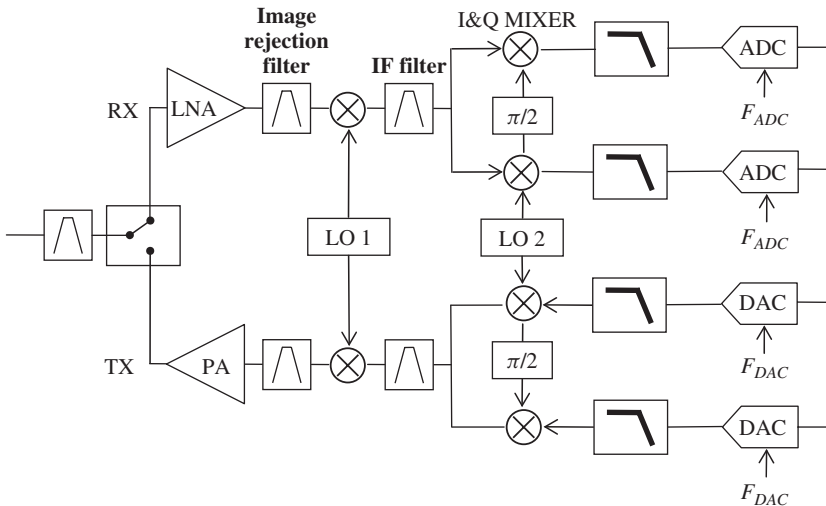


**Figure 1.9** Superheterodyne transceiver

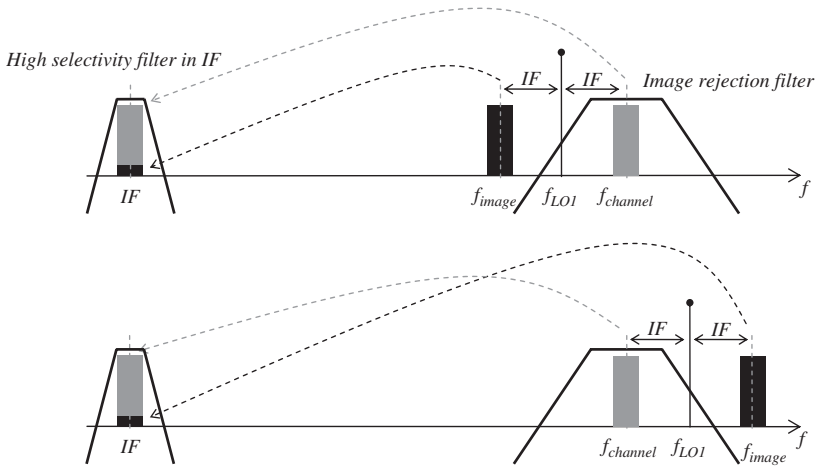


**Figure 1.10** Frequency down-conversion in IF and frequency image issue

to the desired RF channel frequency with the second LO. Before the PA an image rejection filter is necessary in order to attenuate the image before the antenna.

Although the superheterodyne architecture is very well known and presents interesting advantages like high selectivity and limited LO leakage/pulling, it is not appropriate for on-chip integration because of its complexity (two LOs) and the number of components which are prohibitive in low-cost solutions. For example, the two bandpass filters (image rejection and IF) are difficult to integrate on-chip because they require high quality factor components not easily obtained in CMOS technology.

An alternative for limiting the use of discrete analog components is to digitize the real bandpass channel at IF and to perform the quadrature frequency down-conversion and up-conversion to baseband in digital. The superheterodyne architecture with digital IF is presented in Figure 1.11. We can note that this transceiver requires only one DAC and one ADC. The main motivation of this architecture is to avoid the analog IF filter which is very difficult to integrate on-chip. The complexity of this architecture is now dominated by the ADC performance because it has to handle signal levels which include the adjacent channels and to sample the signal at higher frequency (IF), meaning high dynamic-range requirements and more sensitivity to clock jitter. In addition, this architecture still requires an image rejection filter between the LNA and the mixer which is difficult to integrate on-chip at low cost. An option is to increase the IF in order to relax the image rejection filter order, but in this case the DAC and ADC specifications become even more stringent. Consequently, like the classical superheterodyne, this digital IF architecture is not really suitable for low-cost solution integration in CMOS.

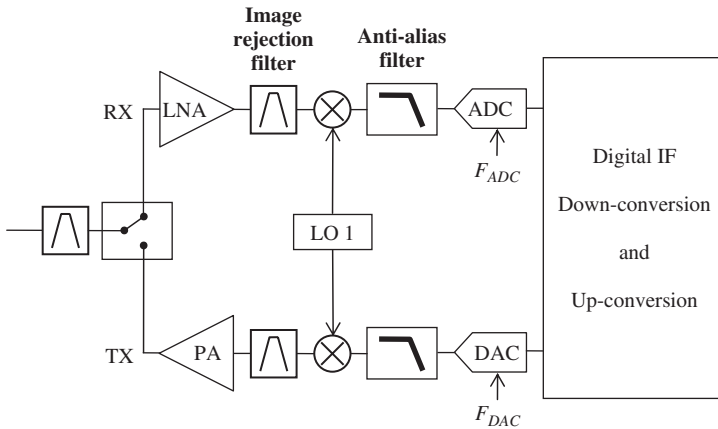


**Figure 1.11** Superheterodyne architecture with digital IF

### 1.2.3 Homodyne Transceiver

A block diagram of the homodyne transceiver (Tucker, 1954) is depicted in Figure 1.12. It is also known as a zero-IF transceiver. The major difference with the superheterodyne transceiver is that the channel, that is, the desired signal, is directly frequency down-converted to baseband in reception, or frequency up-converted to RF in transmission, without using an IF, as shown in Figure 1.13. It is for that reason the homodyne

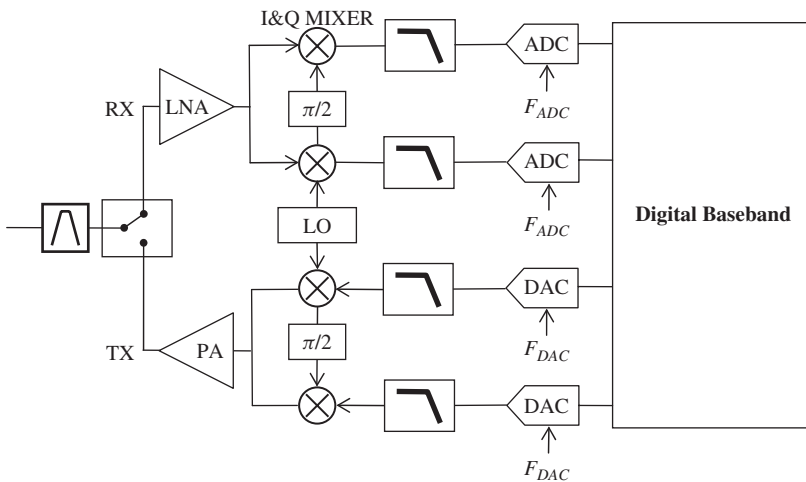


**Figure 1.12** Homodyne or zero-IF architecture

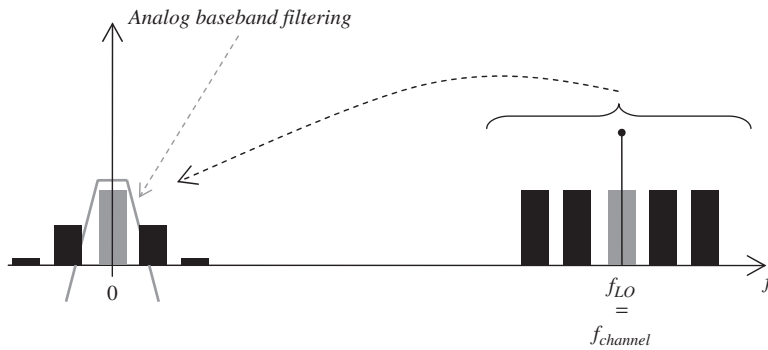


**Figure 1.13** Frequency down-conversion to DC in homodyne or zero-IF architecture

architecture is also called a direct conversion transceiver, because the LO is directly tuned to the desired channel frequency.

Because there is no IF, the RF image rejection filters and the IF bandpass filters are not necessary anymore, thus simplifying the architecture. Consequently, zero-IF architecture is a good candidate for SoC integration (Abidi, 1995; Razavi, 1997); however, different drawbacks exist in both transmission and reception, especially due to LO leakage. Because in reception the baseband signal is centered on DC, it is very sensitive to DC offset coming from the LO self-mixing and baseband active devices. The DC offset can be considerable compared with the desired signal and can therefore severely affect the dynamic range requirements of the baseband path. Regarding on-chip integration, we will see in the next chapter that flicker noise, especially in CMOS, can also limit the performance of narrow-band receivers.

In transmission, the LO leakage into the channel and the LO pulling due to the PA output can be serious performance bottlenecks.

#### 1.2.4 Low-IF Transceiver

As we have previously seen, the zero-IF architecture is a good option for SoC integration but suffers from DC offset issues in reception and LO leakage sensitivity in transmission because the LO and the signal are at the same frequency. One solution is to use a low-IF architecture in which the LO is slightly shifted compared with the channel (Crols and Steyaert, 1998). Low-IF architecture is similar to the zero-IF one depicted in Figure 1.12. The main difference is the fact that the desired channel is offset from DC, requiring wider analog baseband filters than the channel bandwidth, as illustrated in Figure 1.14 for the receiver case. It is interesting to note in this figure that the neighboring channels are included in the baseband band power, which will impact the ADC dynamic range and the AGC. The channel selection is done in digital, where the DC offset is also removed.

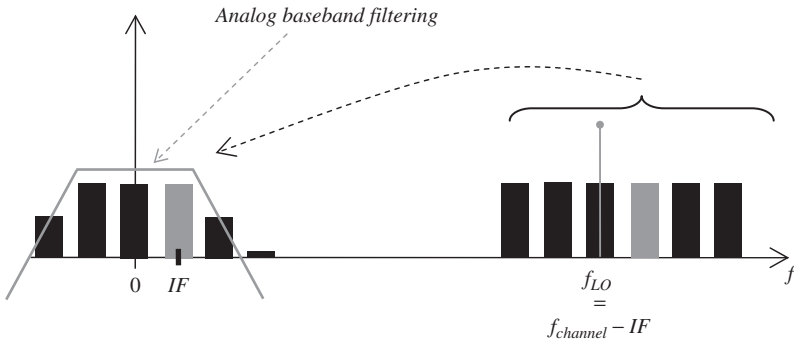


**Figure 1.14** Frequency down-conversion to IF in low-IF architecture

### 1.2.5 Analog Baseband Filter Order versus ADC Dynamic Range

One of the chronic questions for die area and power reduction in the design of CMOS AFEs is the trade-off in reception between the analog baseband filtering order and the ADC dynamic range (Figure 1.15).

By using a high-order analog baseband filter, the out-of-band blockers and interferers are attenuated before the ADC, as illustrated in the Figure 1.16a. The major part of the channel selectivity is achieved in analog and the ADC dynamic range can be optimized for the required signal-to-noise plus distortion ratio (SNDR). In this case the design constraints are especially put on the analog baseband filtering.

In modern transceiver architectures, high dynamic range ADCs allow the use of lower filter orders, in which case the power of the blockers contributes more at the ADC input. As we can see in the Figure 1.16b, the signal is squeezed because the receiver gain must be adjusted based on the blockers strength. In addition we have to be careful about the receiver linearity and noise figure in order to always guarantee the required SNDR. In these new transceiver architectures, the selectivity is especially provided by the DSP.

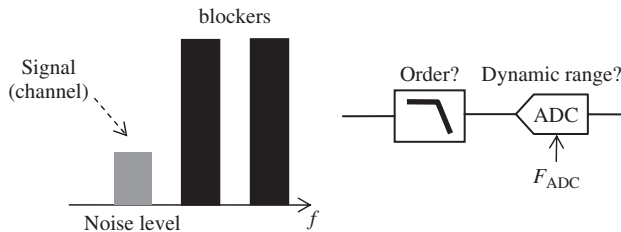


**Figure 1.15** Trade-off between analog baseband filter order and ADC dynamic range

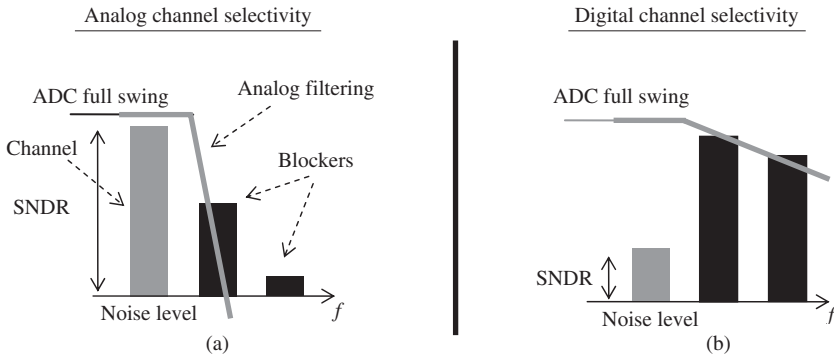


**Figure 1.16** Analog baseband filter order impact on the receiver ADC dynamic range

Another point to take into consideration is the sampling of the analog baseband signal as part of the digitization by the ADC. Indeed, aliasing occurs if spectral components are present above half of the sampling frequency, as demonstrated by the Nyquist–Shannon sampling theorem.

Because the signal of interest is located at baseband, the components around  $nF_s$  will be aliased within the channel as depicted in Figure 1.17. Consequently, the analog baseband filtering must not only be dimensioned as a function of the ADC dynamic range as discussed earlier, but also to limit the aliasing of blockers and noise located at multiples of the ADC clock frequency into the DBB.

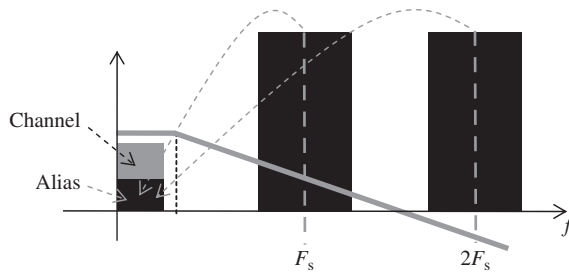


**Figure 1.17** Blockers aliasing before the ADC vs. analog baseband filtering order

### 1.2.6 Digital Compensation of RF Analog Front-End Imperfections

As we have seen in Section 1.1.2, the integration of the RF AFE on-chip is a key point for providing low-cost solutions by reducing the number of chips and saving power in modern mobile handheld devices. Today, CMOS technology is the best candidate for low-cost SoC development but is more adapted to digital design and not really optimized for analog design. In addition, the trend of new

digital telecommunication standards to deliver higher data-rates to the user requires high-performance transceivers, especially for the RF AFE in terms of noise, linearity, matching, and so on. As a result the RF analog impairments pose a serious bottleneck to the integration (Fettweis *et al.*, 2007).

In order to overcome this issue, system designers need to deeply study and understand the impact of the RF AFE impairments on the system performance in order to quantify their impact. The aim is to see if the most severe can be compensated with DSP in order to relax the RF AFE specifications and to integrate it at low cost.

## 1.3 OFDM Modulation

### 1.3.1 OFDM as a Multicarrier Modulation

Orthogonal frequency division multiplexing (OFDM) is a multicarrier modulation increasingly used in communication systems (WiFi, WiMAX (Worldwide Interoperability for Microwave Access), 4G/LTE, power line communication (PLC)) because it presents several advantages compared with single carrier modulation and classical frequency division multiplexing (Bingham, 1990; Van Nee and Prasad, 2000; Prasad, 2004; Li and Stuber, 2006; Armstrong, 2007):

- Efficient use of the spectrum because subcarrier orthogonality allows overlap.
- Less sensitive to channel fading (multipath).
- Channel estimation and equalization in the frequency domain carries low complexity.
- In frequency-selective fading possibility to avoid the affected subcarriers or to adapt their modulation as a function of their SNR.
- Possibility to avoid inter-symbol interference (ISI) with a cyclic prefix.
- Narrow band interferers will only affect few subcarriers.
- Coexistence with other systems: subcarriers can be turned on/off.

However, the use of OFDM modulation presents some drawbacks which have to be taken into account during the system design and specification, such as:

- Very sensitive to frequency and phase offsets and timing error:
  - Break the orthogonality between subcarriers.
- OFDM temporal signal has a high peak to average power ratio (PAPR):
  - Poor efficiency of the PAs.
  - Signal clipping and distortion degrades the SNR and generates out-of-band emissions.

Figure 1.18 schematically describes the principle of OFDM modulation and demodulation, in baseband with subcarriers around DC, using an inverse Fourier transform (IFT) in transmission and a Fourier transform (FT) in reception.

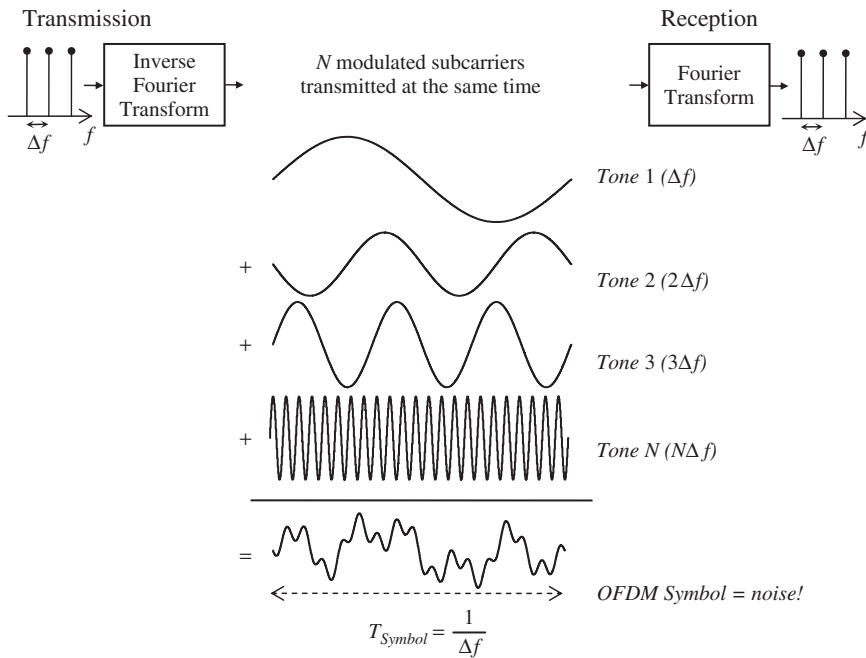


**Figure 1.18** Basic principle of OFDM transmission and reception (baseband illustration)

In transmission, the data are modulated (or mapped) onto  $N$  subcarriers at the input to the IFT which generates an OFDM baseband symbol in the time domain whose duration is inversely proportional to the subcarrier spacing. Because the OFDM symbol is composed of a large number of modulated subcarriers, it looks like a Gaussian noise process in the temporal domain under the central limit theorem, thus explaining its high PAPR.

In reception, after time synchronization to find the beginning of the OFDM symbols, an FT is applied for recovering the subcarriers and then demodulating the data. In reality the subcarriers received are distorted in amplitude and phase by a real transmission channel; as a result channel estimation and equalization are needed for compensating the FT output result before data demodulation.

### 1.3.2 Fourier Transform and Orthogonal Subcarriers

As we have seen in the previous section, the OFDM modulation is performed using the FT mathematical operator (Weinstein and Ebert, 1971). Figure 1.19 is a review of basic FT properties which are necessary to bear in mind for understanding the OFDM modulation principle.

Because OFDM subcarriers are generated during a limited duration  $T$ , or equivalently infinite sine waves multiplied by a rectangular window in the time domain, the result

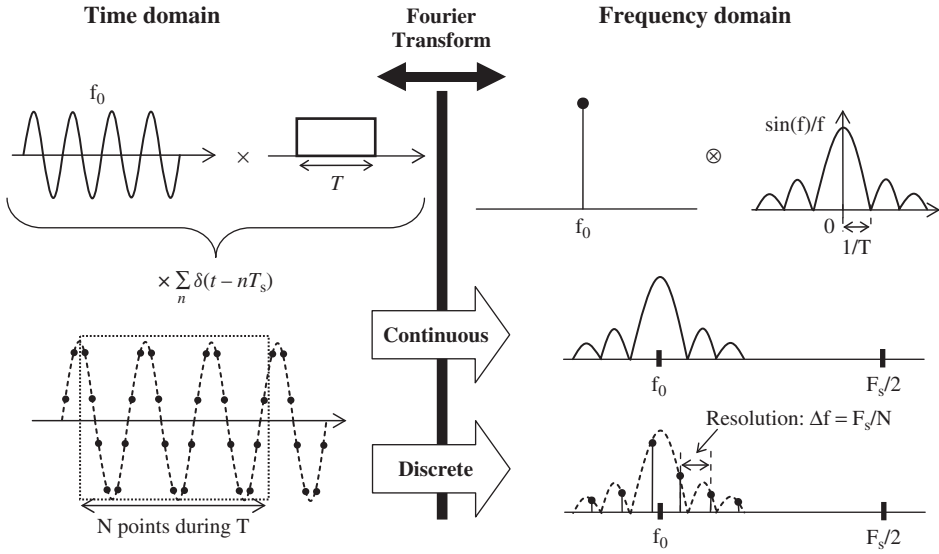


**Figure 1.19** Fourier transform properties important in OFDM

in the frequency domain is a convolution of a zero-width delta function (the spectrum of the infinite-time subcarriers) by the FT of the rectangular window, which is merely a sinc function. The continuous FT of the OFDM symbol  $s(t)$  is given by

$$s(t) = w(t) \times \sum_k s_k e^{j2\pi k \Delta f t} \xleftrightarrow{\text{FT}} S(f) = \int_t s(t) e^{-j2\pi f t} dt \tag{1.1}$$

which can be decomposed as a convolution product:

$$S(f) = \int_t w(t) e^{-j2\pi f t} dt \otimes \int_t \sum_k s_k e^{j2\pi k \Delta f t} e^{-j2\pi f t} dt \tag{1.2}$$

giving

$$S(f) = W(f) \otimes \sum_k s_k \delta(f - k \Delta f) = \sum_k s_k W(f - k \Delta f) \tag{1.3}$$

in which  $w(t)$  and  $W(f)$  are the window responses in the time and frequency domains, respectively,  $\delta()$  is the Dirac function,  $\otimes$  is the convolution operator,  $s_k$  is the complex symbol modulating subcarrier  $k$ , and  $\Delta f$  is the subcarrier spacing.

If  $w(t)$  is a rectangular window having a duration  $T$ , defined between  $-T/2$  and  $T/2$ , we can rewrite Equation 1.3 as

$$S(f) = T \sum_k s_k \frac{\sin[\pi(f - k \Delta f)T]}{\pi(f - k \Delta f)T} \tag{1.4}$$

Equation 1.4 shows that a sinc function, introduced by the FT of the rectangular window, is centered on each modulated subcarrier. The final spectrum is merely the sum of all these shifted and scaled sinc functions.

Because the OFDM transceiver uses a discrete Fourier transform (DFT) applied on  $N$  samples, defined by the number of subcarriers, Equation 1.1 becomes

$$s(nT_s) = s(t) \times \sum_{n=0}^{N-1} \delta(t - nT_s) \xrightarrow{\text{DFT}} S\left(\frac{m}{NT_s}\right) = \frac{1}{N} \sum_{n=0}^{N-1} \sum_{k=-N/2}^{N/2-1} s_k e^{j2\pi k \Delta f n T_s} e^{-j\frac{2\pi}{N} m n} \quad (1.5)$$

in which  $T_s$  is the sampling period and  $m$  is the DFT frequency bin index.

For more clarity in the following development, we rewrite Equation 1.5:

$$S\left(\frac{m}{NT_s}\right) = \frac{1}{N} \sum_{k=-N/2}^{N/2-1} s_k \sum_{n=0}^{N-1} e^{-j\frac{2\pi}{N}(m-kN\Delta f T_s)n} \quad (1.6)$$

By using the result of the geometric series

$$\sum_{n=0}^{N-1} z^{-n} = \frac{1 - z^{-N}}{1 - z^{-1}} \quad (1.7)$$

we can develop Equation 1.6

$$\begin{aligned} S\left(\frac{m}{NT_s}\right) &= \frac{1}{N} \sum_{k=-N/2}^{N/2-1} s_k \frac{1 - e^{-j2\pi(m-kN\Delta f T_s)}}{1 - e^{-j\frac{2\pi}{N}(m-kN\Delta f T_s)}} \\ &= \sum_{k=-N/2}^{N/2-1} s_k \frac{\sin\left[\pi(m-kN\Delta f T_s)\right]}{N \sin\left[\frac{\pi}{N}(m-kN\Delta f T_s)\right]} e^{-j\pi\left(\frac{N-1}{N}\right)(m-kN\Delta f T_s)} \end{aligned} \quad (1.8)$$

In order to ease the study of Equation 1.8, the sum can be decomposed into two components to analyze separately ( $m = k$  and  $m \neq k$ ):

$$S\left(\frac{m}{NT_s}\right) = S_{m=k}\left(\frac{m}{NT_s}\right) + S_{m \neq k}\left(\frac{m}{NT_s}\right) \quad (1.9)$$

$m = k$ : Considered subcarrier

$$S_{m=k}\left(\frac{k}{NT_s}\right) = s_k \frac{\sin\left[k\pi(1 - N\Delta f T_s)\right]}{N \sin\left[\frac{k\pi}{N}(1 - N\Delta f T_s)\right]} e^{-jk\pi\left(\frac{N-1}{N}\right)(1 - N\Delta f T_s)} \quad (1.10)$$

Equation 1.10 shows that all the original symbols  $s_k$  will be distorted in amplitude and in phase depending on the ratio of the subcarrier frequency  $\Delta f$  to the sampling frequency  $F_s = 1/T_s$ .

$m \neq k$ : Inter-carrier interference (ICI)

$$S_{m \neq k} \left( \frac{m}{NT_s} \right) = \sum_{\substack{k=-N/2 \\ m \neq k}}^{N/2-1} s_k \frac{\sin \left[ \pi (m - kN \Delta f T_s) \right]}{N \sin \left[ \frac{\pi}{N} (m - kN \Delta f T_s) \right]} e^{-j\pi \left( \frac{N-1}{N} \right) (m - kN \Delta f T_s)} \quad (1.11)$$

Equation 1.11 shows that all the subcarriers will be distorted by the  $(N - 1)$  others, which is referred to as inter-carrier interference (ICI), and, when present, limits the orthogonality of the OFDM modulation.

In order to obtain orthogonal subcarriers at the DFT output (Equation 1.6) there must be neither subcarrier distortion nor ICI present, which can be mathematically expressed as

$$\begin{aligned} S_{m=k} \left( \frac{k}{NT_s} \right) &= s_k \\ S_{m \neq k} \left( \frac{m}{NT_s} \right) &= 0 \end{aligned} \quad (1.12)$$

The condition for no ICI is

$$\pi (m - kN \Delta f T_s) = n\pi \quad (1.13)$$

for  $m \neq k$  and  $n \neq 0$ , which is satisfied for

$$N \Delta f T_s = 1 \Rightarrow \Delta f = \frac{1}{NT_s} \quad (1.14)$$

Equation 1.14 indicates that the subcarriers are orthogonal if their frequencies are integer multiples of the DFT frequency resolution. In practice, this means that when the DFT computes the considered subcarrier  $k$ , that is,  $m = k$ , the nulls of the sinc function are perfectly aligned with the other subcarriers, producing no ICI.

The previous equations establishing the condition to obtain subcarrier orthogonality are visually summarized in Figure 1.20. We can clearly see the DFT weighting function and the ICI effect if the subcarriers are not multiples of the DFT frequency resolution.

We will see in the subsequent chapters that the RF analog impairments such as sampling and carrier frequency offsets will violate this condition.

### 1.3.3 Channel Estimation and Equalization in Frequency Domain

An important factor affecting the communication systems performance is the propagation channel between the transmitter and the receiver. In wireless communications the signal is received several times with different delays and strengths due to the multipath reflection, and can also be frequency shifted because of the Doppler effect. From a

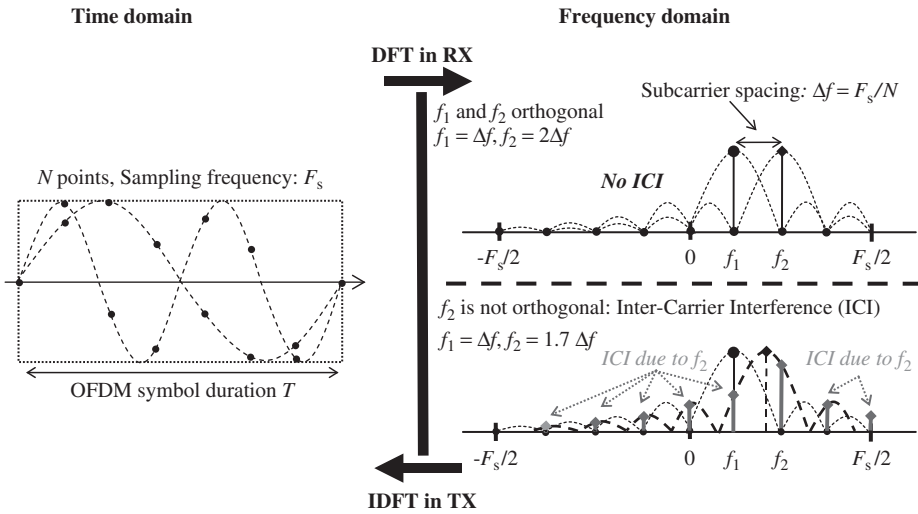


**Figure 1.20** Subcarrier orthogonality and ICI in OFDM

signal processing point of view, the received signal is the result of the convolution of the transmitted signal by the channel impulse response:

$$y(t) = x(t) \otimes h(t) = \int_{\tau} x(\tau)h(t - \tau) d\tau \tag{1.15}$$

where  $y(t)$  and  $x(t)$  are the received and the transmitted signals, respectively,  $h(t)$  is the channel impulse response, and  $\otimes$  is the convolution operator.

Consequently, before the data demodulation the receiver has to compensate the signal distortion due to the channel; it is performed through channel estimation and equalization. Whereas in classical single-carrier systems the channel estimation and equalization have to deal with the convolution of the signal by the channel in time domain, OFDM receivers transform this convolution into multiplication with the FT (Van de Beek *et al.*, 1995; Morelli and Pun, 2007):

$$y(t) = \int_{\tau} x(\tau)h(t - \tau) d\tau \xrightarrow{\text{Fourier transform}} Y(f) = X(f) \times H(f) \tag{1.16}$$

in which  $Y(f)$ ,  $X(f)$ , and  $H(f)$  are the spectra of  $y(t)$ ,  $x(t)$ , and  $h(t)$ , respectively.  $H(f)$  is also called a channel transfer function.

We clearly see in Equation 1.16 the advantage of the channel estimation in frequency domain because the temporal deconvolution to extract the channel is transformed into a simple division:

$$H(f) = \frac{Y(f)}{X(f)} \tag{1.17}$$

On the other hand,  $X(f)$  has to be deterministic so as to be able to estimate the channel transfer function  $H(f)$ . In reality, the receiver uses training sequences or known symbols (pilot-tones) sent by the transmitters before the data in order to estimate the channel amplitude and phase. The zero-forcing equalization (Karp *et al.*, 2002) consists of a division of the fast Fourier transform (FFT) output by the channel estimation:

$$X(f) = \frac{Y(f)}{H(f)} \quad (1.18)$$

Although zero-forcing equalization is straightforward and simple to implement in OFDM, it presents a serious limitation when the channel transfer function  $H(f)$  approaches zero due to deep frequency-selective fading. In this case Equation 1.18 tends to infinity, resulting in a large amplification of the noise, which can create numerical instability (Karp *et al.*, 2003). A solution is to bound the channel transfer function amplitude  $H(f)$  when deep fadings are present; this is the principle of the minimum mean square error (MMSE) criterion equalizer (Farrukh *et al.*, 2009).

#### 1.3.4 Pilot-Tones

In order to aid the receiver in estimating the propagation channel and to correct transceiver impairments such as carrier frequency and sampling clock offsets between transmitter and receiver, deterministic subcarriers are sent by the transmitter (Figure 1.21). These carriers are called pilots (Hoeher *et al.*, 1997; Tufvesson and Maseng, 1997). Knowing their properties, that is, their frequencies and their phase and amplitude, the receiver can exploit them in order to extract the phase and amplitude of the channel to be used by the equalizer to compensate the output of the FFT. Because the demodulated data quality strongly depends on the channel estimation precision, the demodulation of the pilots has to be robust. Consequently, they are generally boosted in power a few decibels above the subcarriers used for data.

Because the pilots are much less than the total number of subcarriers, the channel estimation for all the subcarriers is performed using interpolation methods.

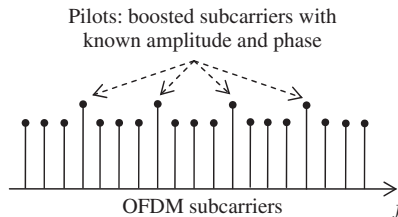


**Figure 1.21** Pilot-tones used in reception for channel estimation

It is also possible to track the channel in time and frequency by moving the pilot positions between OFDM symbols.

### 1.3.5 Guard Interval

In communication systems the multipath reflections due to signal propagation create channel delay spread which can severely affect receiver demodulation performance. This is known as ISI. Whereas in single-carrier systems it can be a serious bottleneck, in OFDM transmission it is possible to add a guard interval, also called a cyclic prefix, between the symbols in order to “absorb” this channel delay spread. The guard interval insertion consists of copying the last samples of the OFDM symbol and pre-pending them to the front of the symbol as illustrated in Figure 1.22. The length of the guard interval is adjusted to the maximum expected delay spread of the channel to allow the receiver to perform the FFT without ISI.

On the other hand, the addition of a guard interval reduces the system data-rate because the time duration of the OFDM symbol is increased while the number of transmitted bits remains the same.

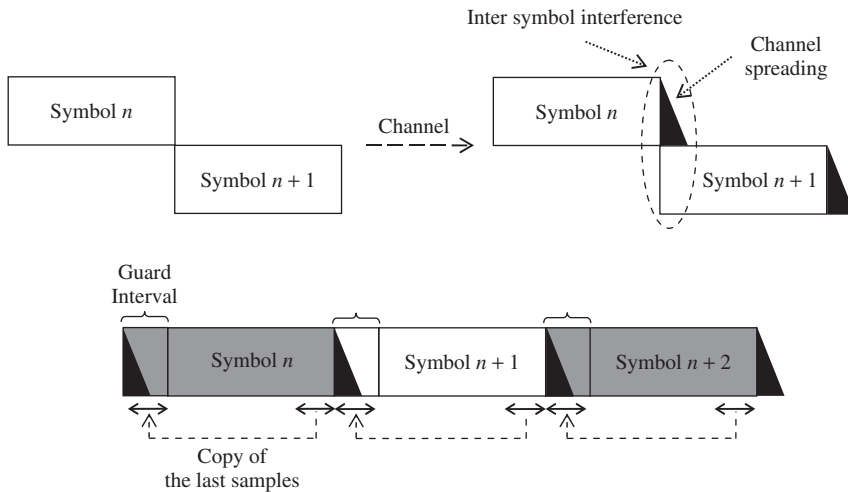


**Figure 1.22** Guard interval insertion in order to combat the channel delay spread and the ISI

### 1.3.6 Windowed OFDM

Recent OFDM transceivers use windowing in transmission in order to reduce out-of-band emissions and to achieve deeper notches around unused subcarriers. The idea is to smooth the transition between OFDM symbols as opposed to the classical rectangular

window shape whose frequency response is a sinc ( $\sin(f)/f$ ) function, Equation 1.4), which provides a spectral roll-off of only  $-20$  dB/decade. Because the windowing reduces the effective guard interval used for combating the ISI, it has to be carefully adjusted for large channel delay spreads.

Figure 1.23 shows how the windowed OFDM shapes the OFDM symbol in the time domain, along with its impact on the power spectral density (PSD).

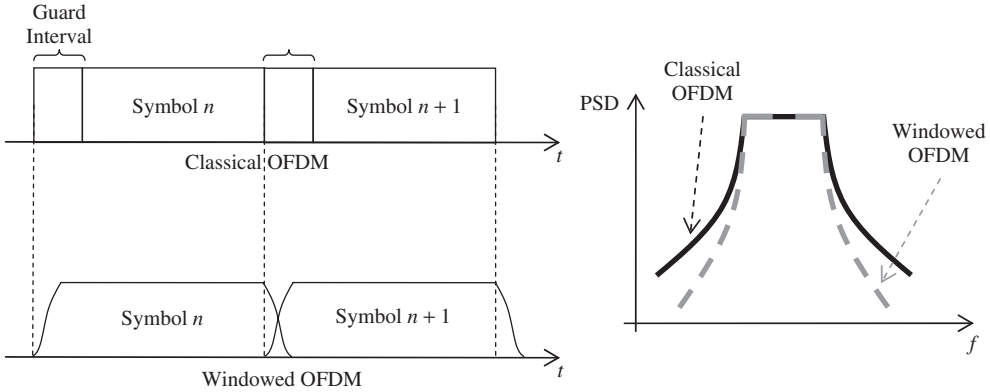


**Figure 1.23** Windowed OFDM reduces the out-of-band emissions of the OFDM transmitter

### 1.3.7 Adaptive Transmission

Another very interesting feature of OFDM modulation is the capability to adapt the modulation per subcarrier, or per sub-channel, as illustrated in Figure 1.24. Because the channel is estimated in the frequency domain, after the FFT, it is possible to obtain the SNR per subcarrier and thus adapt the modulation order as a function of the channel properties. For example, if a 64-quadrature amplitude modulation (QAM) modulated subcarrier is suddenly attenuated due to a deep frequency-selective fading, it is better to lower its modulation to 16-QAM or 4-QAM in order to continue reliably transmitting data, rather than lose the information due to the inability to demodulate

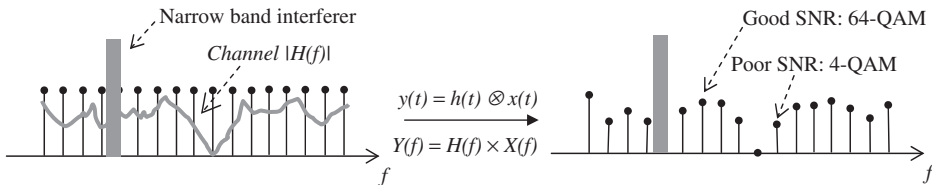


**Figure 1.24** Subcarrier adaptive modulation

64-QAM. In addition, the OFDM receiver can detect narrow-band interferers and blank the affected subcarriers.

This technique is only achievable if the receiver is able to send the channel properties to the transmitter such that the transmission can be optimized or adapted to the link quality.

### 1.3.8 OFDMA for Multiple Access

Whereas in classical OFDM transceivers all the subcarriers of the OFDM symbols are allocated to one user per OFDM symbol, orthogonal frequency division multiple access (OFDMA) divides the subcarriers into sub-channels (Yang, 2010). The concept is to simultaneously share the same OFDM symbol, that is, the channel, between several users at the same time (Figure 1.25). Consequently, in OFDMA all the users receive information about the position of their sub-channel within the OFDM symbol. OFDMA also uses frequency diversity between the users in order to limit the impact of frequency-selective fading which can affect only certain sub-channels, that is, particular subcarriers. OFDMA can resourcefully control the data-rate of each user by adapting the number of allocated subcarriers.

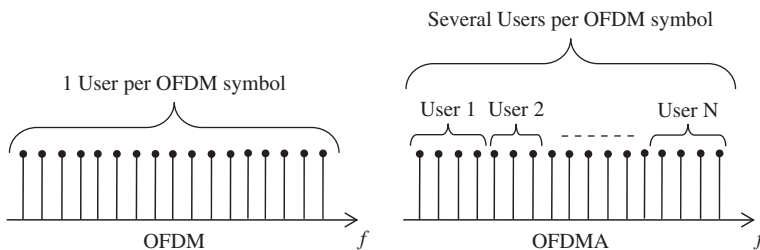


**Figure 1.25** In OFDMA the subcarriers of one OFDM symbol are shared between several users

### 1.3.9 Scalable OFDMA

Because spectrum allocation is imposed by the regulatory rules of each country as well as the network operators, new standards like 3GPP LTE or mobile WiMAX have introduced scalable orthogonal frequency division multiple access (S-OFDMA) in order to be able to customize the OFDMA channel bandwidth (Yang, 2010). However, if the number of subcarriers is not adapted to the channel bandwidth, that is, constant, the system performance will be dependent on the latter. Indeed, narrowing the OFDMA channel bandwidth results in smaller subcarrier spacing and consequently the system becomes more sensitive to Doppler shift, phase noise, and frequency errors, impacting the system specification and complexity. Conversely, if the channel bandwidth is increased, the spectral efficiency lowers because the subcarrier spacing maybe overspecified.

The principle of S-ODFMA is to scale the number of subcarriers with the channel bandwidth in order to keep the subcarrier spacing constant and independent of the system bandwidth.

### 1.3.10 OFDM DBB Architecture

Figure 1.26 gives an overview of the DBB of a typical OFDM transceiver, which can be decomposed in three separate domains:

- *The bit processing, where the information coming from the MAC is coded and decoded using a forward error correction (FEC) coding.*

The aim of the channel coding, also called FEC, is to add coded redundant bits to the useful bit stream in order to be more robust to channel fading and noise. The channel decoder at reception uses this redundancy for detecting errors and is able to correct them if the SNR is high enough. The coding rate specifies the ratio between the useful bits and the total number of bits that the code generates. For example, a coding rate of  $1/2$  means that the channel coding output is 2 bits for every useful bit at the input; that is, we have one redundant bit. If  $D$  is the PHY data rate including the coding bits, the useful data rate is obtained by multiplying  $D$  by the coding rate, giving half of the PHY data rate for a coding rate of  $1/2$ . The efficiency of the coding is generally quantified using bit-error-rate (BER) curves as a function of  $E_b/N_0$ , where the best achievable performance is given by the Shannon limit.

Because communication channels introduce bursts of errors causing degradation of several consecutive bits in the data stream, the efficiency of the channel coding alone is not optimal, as it assumes independent errors spread over the bit stream. As a result, interleaving and deinterleaving techniques have been introduced for randomizing the bit ordering between the transmitter and the receiver, and thus also the position of errors at the input of the decoder. This allows an improvement in the performance of the channel coding.

- *The frequency-domain processing, where the bits are represented in a complex plane as symbols used to modulate the OFDM subcarriers.*

In transmission, after the channel coding the symbol mapping transforms the bit stream into constellation points. The complexity of the constellation depends on the modulation order. Figure 1.27 shows the mapping for 16-QAM. The constellation points define the magnitudes and the phases of the symbols to apply to the subcarriers before the inverse fast Fourier transform (IFFT) (Figure 1.28).

At the receiver, after the FFT the phase and magnitude of each carrier are extracted and a decision must be taken about which symbol was sent by the transmitter. Due to the channel response each carrier has been distorted in phase and in amplitude, introducing errors in the position of the received constellation points. Consequently, before the symbol demapping, an algorithm is used for estimating the channel response which

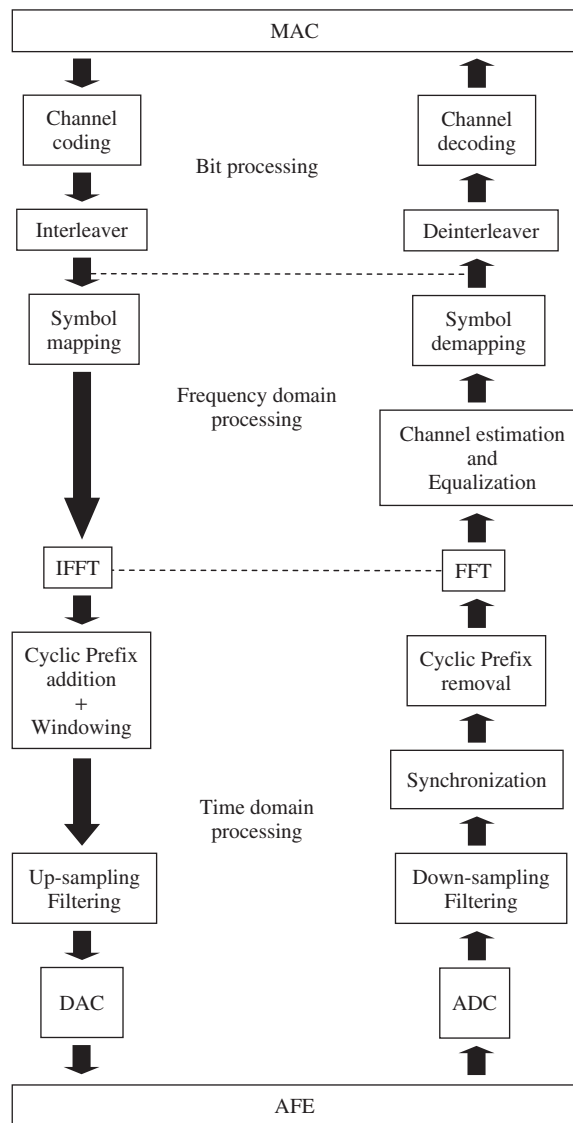


**Figure 1.26** OFDM DBB Overview

can be represented in the frequency domain by a phase and an amplitude as a function of subcarrier position. Generally, the channel estimation is performed using training sequences sent by the transmitter or known subcarriers called pilots. Afterwards, the channel estimate is utilized to equalize (i.e., remove the distortion introduced by the channel) all the subcarriers before the symbol demapping, which finally extracts the bit stream from the received equalized constellation. Other algorithms are also used in the

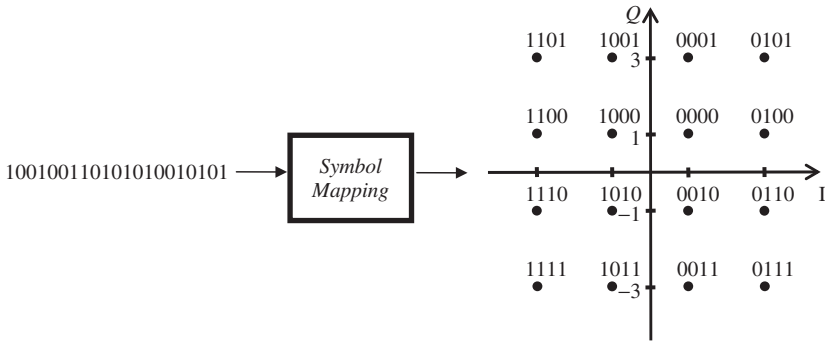


**Figure 1.27** Symbol mapping transforms the bit stream into a complex constellation, here 16-QAM

frequency domain for tracking and compensating the carrier and sampling frequency offsets which introduce deterministic phase rotation.

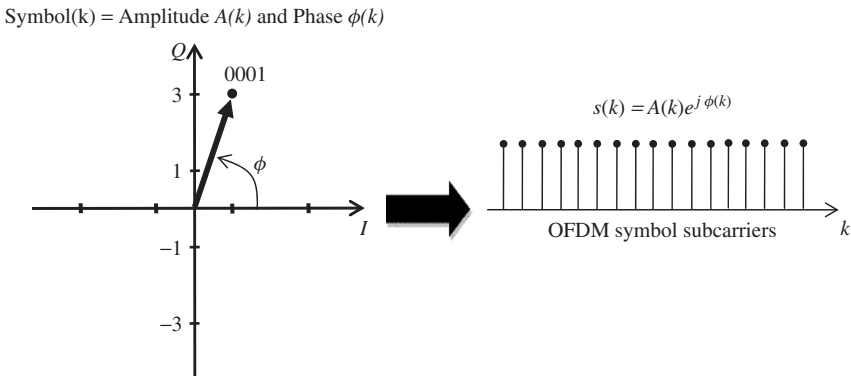


**Figure 1.28** The constellation points determine the amplitude and the phase of the subcarriers

- *The time-domain processing after the IFFT in transmission and before the FFT in reception.*

In transmission, after the IFFT the data is now in the time domain where the cyclic prefix is added, which determines the guard interval, and windowing is performed on the OFDM symbol. Finally, up-sampling and digital filters can be used if the DAC clock frequency is higher than the assumed IFFT sampling rate.

In reception, down-sampling and digital filtering can be present if the ADC clock frequency is different than the assumed FFT sampling rate. Time synchronization is

required in order to find the precise instants when the OFDM symbols start before applying the FFT. This synchronization can be made, for example, using a known sequence sent by the transmitter or via an autocorrelation using the cyclic prefix and the end of the OFDM symbol.

### 1.3.11 OFDM-Based Standards

Today, many communication standards use OFDM as modulation for their PHY, notably due to its robustness in the presence of severe channel conditions, as well as its low-complexity equalization done in the frequency domain, which is much simpler than the time-domain equalization used in conventional single-carrier modulation.

The first OFDM-based standards were introduced in the mid 1990s by ETSI (European Telecommunications Standard Institutes) for Digital Audio Broadcasting (DAB) and Digital Video Broadcasting (DVB-T, T for terrestrial). Fifteen years later many others have been developed and are now operational, either for wireless or cable, including:

- Wireless:
  - WiFi (wireless fidelity) for wireless local area networks (WLANs): IEEE 802.11a, g, n.
  - The mobility mode of the IEEE 802.16 wireless metropolitan area networks (WMANs) mobile-WiMAX: IEEE 802.16e based on S-OFDMA.
  - The fourth-generation mobile broadband standard: 3GPP LTE based on S-OFDMA.
  - The terrestrial mobile TV: DVB-H (Digital Video Broadcasting-Handheld).
- Cable:
  - ADSL (asymmetric digital subscriber line) and VDSL (very-high-bit-rate digital subscriber line) for high-definition TV and Internet access over copper phone wires.
  - PLC: Home Plug AV, IEEE 1901, ITU-T G.hn.
  - Multimedia Over Coax Alliance for home networking: MoCA.

## 1.4 SNR, EVM, and $E_b/N_0$ Definitions and Relationship

### 1.4.1 Bit Error Rate

In order to quantify the performance of communication systems, we often find in the literature the use of a BER metric giving the probability of error in terms of the number of corrupted bits per bits received (Proakis, 1995). Depending on the application the BER target can vary from  $10^{-3}$  to  $10^{-15}$ , that is, one erroneous bit every 1000 or  $10^{15}$  bits, respectively. Consequently, the system simulations for measuring these very low BER levels are generally time consuming and cumbersome because large amounts of data, several millions of bits, have to be processed using an accurate model of the DBB chain.

Because the AFE is composed of several blocks (LNA, phase-locked loop (PLL), mixer, etc.) designed by different engineers, it is not practical to directly use the BER as a specification. RF analog designers prefer to work with SNR and/or EVM as performance metrics for specifying and designing the AFE blocks. So it is important that the system designer be able to translate the BER target into SNR or EVM specifications for the AFE development. One technique is to extract the required SNR or EVM from the BER curves, but as they are commonly represented as a function of  $E_b/N_0$ , a relationship between these various performance metrics is needed.

Figure 1.29 is a plot of BER curves as a function of  $E_b/N_0$  for four different modulations: 4-QAM, 16-QAM, 64-QAM, and 1024-QAM. If the goal is to achieve a BER lower than  $10^{-6}$ , we clearly see that 1024-QAM requires a much higher  $E_b/N_0$  than 4-QAM, approximately 18dB higher. With this illustration we can imagine why high data-rate communication systems using high-order modulations need high-performance transceivers, resulting in increased design complexity and increased costs of the final solutions.

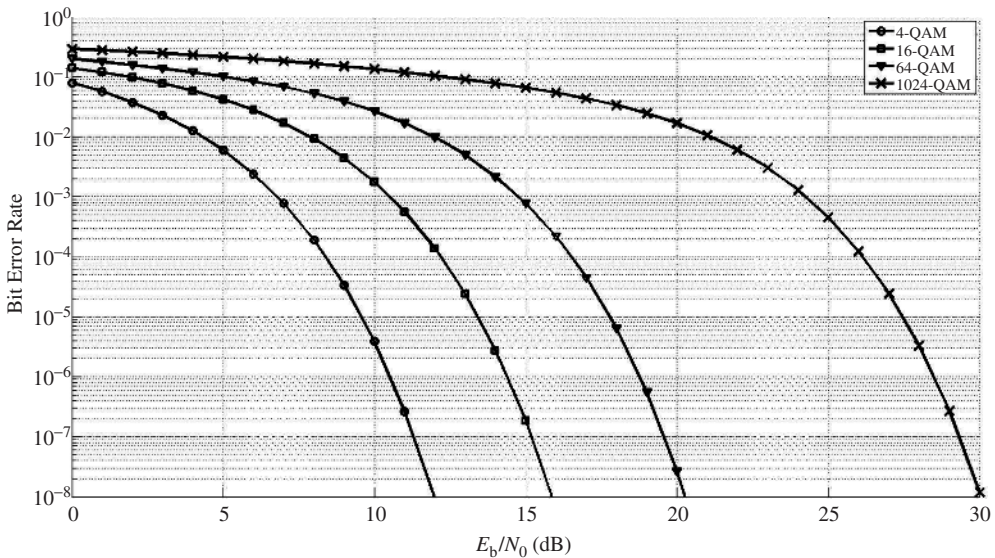


**Figure 1.29** BER vs.  $E_b/N_0$  for 4-QAM, 16-QAM, 64-QAM, and 1024-QAM modulations

### 1.4.2 SNR versus EVM

The SNR is defined as the ratio between the received signal power  $P_s$  and the noise power  $P_n$  integrated within the receiver noise bandwidth  $B$ ; it is used to predict the performance of the system in terms of minimum receiver sensitivity, or the minimum

input signal power which guarantees a certain quality of the communication link.

$$\text{SNR} = \frac{\text{Signal Power}}{\text{Noise Power}} = \frac{P_s}{P_n} = \frac{\frac{1}{T} \int |s(t)|^2 dt}{N_0 B} \quad (1.19)$$

where  $P_s$  and  $P_n$  are the power of the received signal and the power of the noise in watts, respectively.  $N_0$  is the PSD of the noise in watts per hertz.

In modern communication systems using digital  $M$ -ary modulation, the signal is generated using complex symbols:

$$s(t) = x_I(t) + jx_Q(t) \quad (1.20)$$

where  $x_I(t)$  and  $x_Q(t)$  are the in-phase and quadrature components of the signal. If we introduce the in-phase and quadrature components of the additive noise,  $n_I(t)$  and  $n_Q(t)$ , respectively, we obtain the noisy signal:

$$s(t) = x_I(t) + jx_Q(t) + n_I(t) + jn_Q(t) \quad (1.21)$$

and the SNR defined in Equation 1.19 can be expressed as

$$\text{SNR} = \frac{\frac{1}{T} \int |x_I^2(t) + x_Q^2(t)| dt}{\frac{1}{T} \int |n_I^2(t) + n_Q^2(t)| dt} \quad (1.22)$$

Equation 1.22 shows a direct estimation of the SNR which can be computed in simulation for quantifying the system performance. But in simulation, how can one extract the signal from the noise in Equation 1.21 in order to calculate this ratio? It is not at all obvious, especially for OFDM signals which look like noise; that is, not specified in a deterministic way in the time domain.

One solution is to estimate the EVM, which is another performance metric used by RF analog engineers by measuring the modulation accuracy directly on the constellation points after demodulation (Figure 1.30).

The EVM is defined as the root-mean-square (RMS) of the error between the measured symbols  $s_n$  and the ideal ones  $s_{0,n}$ :

$$\text{EVM} = \sqrt{\frac{\frac{1}{N} \sum_{n=1}^N |s_n - s_{0,n}|^2}{\frac{1}{N} \sum_{n=1}^N |s_{0,n}|^2}} \quad (1.23)$$

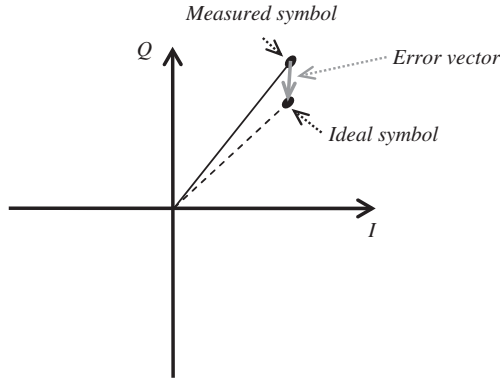


**Figure 1.30** Modulation error vector used for estimating the EVM

which can be rewritten:

$$\text{EVM} = \sqrt{\frac{\frac{1}{N} \sum_{n=1}^N |x_{I,n} - x_{I0,n}|^2 + |x_{Q,n} - x_{Q0,n}|^2}{\frac{1}{N} \sum_{n=1}^N |x_{I0,n}|^2 + |x_{Q0,n}|^2}} \quad (1.24)$$

where  $x_{I,n}$  and  $x_{Q,n}$  are the coordinates of the measured symbols in the complex domain, and  $x_{I0,n}$  and  $x_{Q0,n}$  are those of the ideal ones.

Using Equation 1.21 we can express the noisy symbols as a function of the ideal ones and the quadrature components of an additive noise:

$$\begin{aligned} x_{I,n} &= x_{I0,n} + n_{I,n} \\ x_{Q,n} &= x_{Q0,n} + n_{Q,n} \end{aligned} \quad (1.25)$$

Combining Equations 1.24 and 1.25, the EVM becomes

$$\text{EVM} = \sqrt{\frac{\frac{1}{N} \sum_{n=1}^N |n_{I,n}|^2 + |n_{Q,n}|^2}{\frac{1}{N} \sum_{n=1}^N |x_{I0,n}|^2 + |x_{Q0,n}|^2}} \quad (1.26)$$

which is the square root of the ratio between the noise power and the signal power; that is, the inverse of the SNR:

$$\text{EVM} = \sqrt{\frac{\text{Noise Power}}{\text{Signal Power}}} = \frac{1}{\sqrt{\text{SNR}}} \quad (1.27)$$

Equation 1.27 shows that the SNR can be directly computed from the value of the EVM:

$$\text{SNR} = \frac{1}{\text{EVM}^2} \quad (1.28)$$

giving in decibels:

$$\text{SNR}_{\text{dB}} = 10 \log_{10} \left( \frac{1}{\text{EVM}^2} \right) = -20 \log_{10} (\text{EVM}) \quad (1.29)$$

### 1.4.3 SNR versus $E_b/N_0$

The ratio  $E_b/N_0$ , mainly used in BER simulations, quantifies the ratio between the energy per bit and the PSD of the noise.

The energy per bit is defined as the ratio between the signal power and the bit rate:

$$E_b = \frac{P_s}{R_b} \quad (1.30)$$

in which  $P_s$  is the signal power in watts and  $R_b$  is the data rate in bits/second, giving  $E_b/N_0$  in watt-seconds/bit; that is, joules/bit.

By introducing the noise power, Equation 1.30 can be expressed as a function of the system SNR:

$$E_b = \frac{P_s}{N_0 B} \times \frac{N_0 B}{R_b} = \text{SNR} \times \frac{N_0 B}{R_b} \quad (1.31)$$

in which  $B$  is the equivalent noise bandwidth.

Normalizing Equation 1.31 by the noise spectral density  $N_0$ , we obtain the formula for  $E_b/N_0$  as a function of the SNR, system bandwidth and bit rate:

$$\frac{E_b}{N_0} = \text{SNR} \times \frac{B}{R_b} \quad (1.32)$$

Combining Equations 1.28 and 1.32,  $E_b/N_0$  can also be expressed as function of the EVM:

$$\frac{E_b}{N_0} = \frac{1}{\text{EVM}^2} \times \frac{B}{R_b} \quad (1.33)$$

Equation 1.32 shows that  $E_b/N_0$  and SNR are equivalent if the system bandwidth is equal to the bit rate, meaning that each transmitted bit requires the full system bandwidth. On the other hand, for communication systems using spread spectrum techniques, like code division multiple access (CDMA) in mobile phones or in GPS, the RF analog noise bandwidth  $B$  can be much larger than the information data rate. In practice this means that, after demodulation of the data, each information bit occupies a smaller bandwidth than the RF analog noise bandwidth; the result is a processing gain:

$$\text{PG} = \frac{B}{R_b} \quad (1.34)$$

which can be seen directly as the gain in  $E_b/N_0$  above the SNR in Equation 1.32.

### 1.4.4 Complex Baseband Representation

In general for system simulations we prefer to work with the complex baseband signal in order to avoid the use of high sampling rates imposed by up-conversion to the carrier frequency, which does not convey any additional information.

The conversion from a real bandpass signal to a complex baseband signal is illustrated in Figure 1.31.

Let us write the original baseband signal at the transmitter input as

$$s(t) = x_I(t) + jx_Q(t) \quad (1.35)$$

The transmitter frequency up-converts the complex baseband signal to a real bandpass signal using a quadrature mixer driven by an LO. The real bandpass signal at the transmitter output, including the carrier frequency, is

$$s_{\text{RF}}(t) = \sqrt{2} \operatorname{Re} \{s(t) \times e^{j2\pi F_c t}\} = x_I(t)\sqrt{2} \cos(\omega_c t) - x_Q(t)\sqrt{2} \sin(\omega_c t) \quad (1.36)$$

By assuming an additive noise, the real bandpass signal becomes

$$s_{\text{RF}}(t) = x_I(t)\sqrt{2} \cos(\omega_c t) - x_Q(t)\sqrt{2} \sin(\omega_c t) + n_I(t)\sqrt{2} \cos(\omega_c t) + n_Q(t)\sqrt{2} \sin(\omega_c t) \quad (1.37)$$

$n_I(t)$  and  $n_Q(t)$  being the quadrature components of the baseband noise.

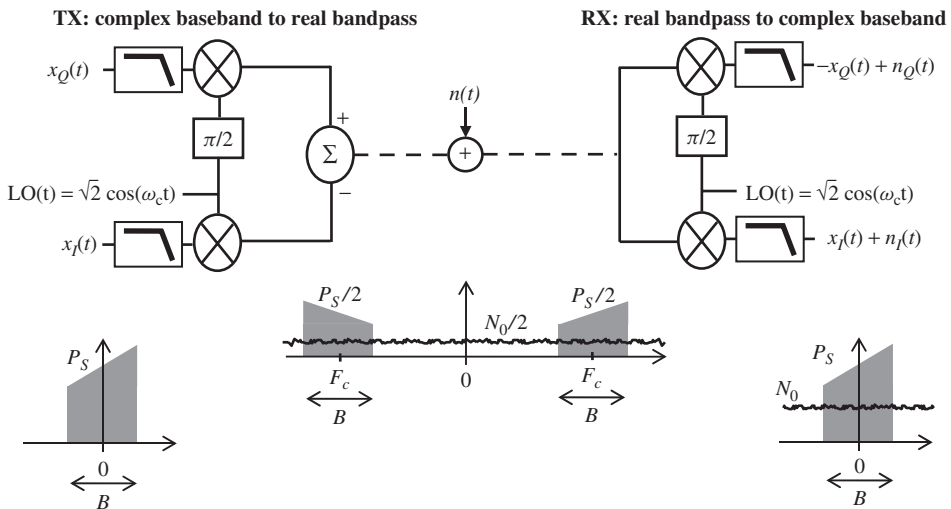


**Figure 1.31** From real bandpass to complex baseband used in system simulations

The SNR at RF is estimated by calculating

$$\text{SNR}_{\text{RF}} = \frac{\left\langle \left[ x_I(t)\sqrt{2}\cos(\omega_c t) - x_Q(t)\sqrt{2}\sin(\omega_c t) \right]^2 \right\rangle}{\left\langle \left[ n_I(t)\sqrt{2}\cos(\omega_c t) + n_Q(t)\sqrt{2}\sin(\omega_c t) \right]^2 \right\rangle} \quad (1.38)$$

If we only consider the signal of interest around the carrier frequency, that is, ignoring the terms at two times the carrier frequency, we obtain

$$\text{SNR}_{\text{RF}} = \frac{\langle x_I^2(t) + x_Q^2(t) \rangle}{\langle n_I^2(t) + n_Q^2(t) \rangle} = \frac{P_s}{N_0 B} \quad (1.39)$$

in which  $P_s$  is the signal power in watts,  $B$  is the noise bandwidth in hertz, and  $N_0$  is the noise spectral density in watts/hertz.

The conversion from real bandpass to complex baseband is done in reception by using a complex frequency down-conversion:

$$\begin{aligned} s_{\text{BB}}(t) = & \left[ x_I(t)\sqrt{2}\cos(\omega_c t) - x_Q(t)\sqrt{2}\sin(\omega_c t) \right. \\ & \left. + n_I(t)\sqrt{2}\cos(\omega_c t) + n_Q(t)\sqrt{2}\sin(\omega_c t) \right] \times \sqrt{2}\cos(\omega_c t) \\ & + j \left[ x_I(t)\sqrt{2}\cos(\omega_c t) - x_Q(t)\sqrt{2}\sin(\omega_c t) \right. \\ & \left. + n_I(t)\sqrt{2}\cos(\omega_c t) + n_Q(t)\sqrt{2}\sin(\omega_c t) \right] \times \sqrt{2}\sin(\omega_c t) \end{aligned} \quad (1.40)$$

After lowpass filtering to remove the high-frequency components around  $2\omega_c$ , we obtain

$$s_{\text{BB}}(t) = (x_I(t) - jx_Q(t)) + (n_I(t) + jn_Q(t)) \quad (1.41)$$

The SNR in baseband is then

$$\text{SNR}_{\text{BB}} = \frac{\langle x_I^2(t) + x_Q^2(t) \rangle}{\langle n_I^2(t) + n_Q^2(t) \rangle} = \frac{P_s}{N_0 B} \quad (1.42)$$

which is strictly equal to the RF SNR of the real bandpass signal defined in Equation 1.39, meaning that performance with respect to additive noise is unchanged and the complex baseband model can be used equivalently to the real bandpass model in system simulations.

We will see in the next chapter that the RF impairments are also translated to equivalent models at complex baseband.

## References

- Abidi, A.A. (1995) Direct-conversion radio transceivers for digital communications. *IEEE Journal on Solid-State Circuits*, **30**, 1399–1410.
- Abidi, A. (2000) Wireless transceivers in CMOS IC technology: the new wave, Proceedings of the Symposium on VLSI Technology, pp. 151–158.
- Armstrong, J. (2007) *OFDM*, John Wiley & Sons, Inc.
- Bingham, J.A.C. (1990) Multicarrier modulation for data transmission: an idea whose time has come. *IEEE Communications Magazine*, **28**, 5–14.
- Brandolini, M., Rossi, P., Manstretta, D., and Svelto, F. (2005) Toward multi-standard mobile terminals – fully integrated receivers requirements and architectures. *IEEE Transactions on Microwave Theory and Techniques*, **53** (3), 1026–1038.
- Crols, J. and Steyaert, M.S.J. (1998) Low-if topologies for high-performance analog front ends of fully integrated receivers. *IEEE Transactions on Circuits Systems II*, **45**, 269–282.
- Farrukh, F., Baig, S., and Mughal, M.J., (2009) MMSE equalization for discrete wavelet packet based OFDM. Proceedings of IEEE International Conference on Electrical Engineering.
- Fettweis, G., Löhning, M., Petrovic, D. *et al.* (2007) Dirty RF: a new paradigm. *International Journal of Wireless Information Networks*, **14** (2), 133–148.
- Haykin, S. (2001) *Communication Systems*, 4th edn, John Wiley & Sons, Inc.
- Hoehner, P., Kaiser, S., and Robertson, P. (1997) Pilot-symbol aided channel estimation in time and frequency. Proceedings of Globecom, pp. 90–96.
- Iwai, H. (2000) CMOS technology for RF applications. *Proceedings of the 22nd International Conference on Microelectronics*, Vol. 1, pp. 27–34.
- Karp, T., Trautmann, S., and Fliege, N.J. (2002) Frequency domain equalization of DMT/OFDM systems with insufficient guard interval. Proceedings of the IEEE International Conference on Communications, pp. 1646–1650.
- Karp, T., Wolf, M., Trautmann, S., and Fliege, N.J. (2003) Zero-forcing frequency domain equalization for DMT systems with insufficient guard interval. Proceedings of IEEE International Conference on Acoustics, Speech, and Signal Processing, pp. 221–224.
- Morelli, M. and Pun, M. (2007) Synchronization techniques for orthogonal frequency division multiple access (OFDMA) a tutorial review. *Proceedings of the IEEE*, **95** (7), 1394–1427.
- Lee, T.H. (1998) *The Design of CMOS Radio-Frequency Integrated Circuits*, Cambridge University Press.
- Li, Y.G. and Stuber, G.L. (2006) *Orthogonal Frequency Division Multiplexing for Wireless Channels*, 1st edn, Springer.
- Prasad, R. (2004) *OFDM for Wireless Communications Systems*, Artech House.
- Proakis, J.G. (1995) *Digital Communications*, McGraw-Hill, New York.
- Rappaport, T.S. (1996) *Wireless Communications: Principles and Practice*, Prentice Hall.
- Razavi, B. (1997) Design considerations for direct conversion receivers. *IEEE Transactions on Circuits and Systems II: Analog and Digital Signal Processing*, **44**, 428–435.
- Razavi, B. (1998a) *RF Microelectronics*, Prentice Hall.
- Razavi, B. (1998b) Architecture and circuits for RF CMOS receivers. Proceedings IEEE Custom Integrated Circuits Conference, pp. 393–400.
- Steele, R. (1995) *Mobile Radio Communications*, IEEE Press.

- Tucker, D.G. (1954) The history of the homodyne and the synchrodyne. *Journal of the British Institution of Radio Engineers*, **14**, 143–154.
- Tufvesson, F. and Maseng T. (1997) Pilot assisted channel estimation for OFDM in mobile cellular systems. Proceedings of Vehicular Technology Conference, pp. 1639–1643.
- Van de Beek, J.J., Edfors, O., Sandell, M. *et al.* (1995) On channel estimation in OFDM systems. Proceedings of Vehicular Technology Conference, pp. 815–819.
- Van Nee, R.D.J. and Prasad, P. (2000) *OFDM for Wireless Multimedia Communications*, Artech House.
- Weinstein, S.B. and Ebert, P.M. (1971) Data transmission by frequency-division multiplexing using the discrete Fourier transform. *IEEE Transactions on Communications*, **19**, 628–634.
- Yang, S.C. (2010) *OFDMA System Analysis and Design*, Mobile Communication Series, Artech House.

